Vol. 7(Iss. 2) 2026, pp.1103-1113, African Journal of Empirical Research https://ajernet.net

Thresholds for Noise-Induced Instability in a Three-Patch Predator-Prey Fishery with Prey Migration

Lucian Talu Mayabi

Department of Mathematics, Masinde Muliro University of Science and Technology
P.O BOX 190-50100, Kakamega, Kenya

* talumayabi@gmail.com

https://doi.org/10.51867/ajernet.maths.7.2.94

Abstract

Understanding how environmental fluctuations affect multi-patch predator-prey systems is critical for sustainable fisheries management. While deterministic and stochastic models have been studied extensively in single-patch or two-patch settings, the combined effect of prey migration and additive white noise on population persistence in a three-patch ecosystem remains largely unexplored. Here we develop a stochastic predator-prey model for three interconnected patches (cages) where prey fingerlings migrate among patches. We derive conditions for stochastic stability using a Lyapunov function and show that the system is stable when the predator conversion efficiency $e_i < 1$ and unstable when $e_i > 1$. Numerical simulations using the Euler-Maruyama scheme reveal clear thresholds: prey populations remain viable only when harvesting rates are maintained below $\nu_i = 0.02$ per patch and noise intensities are kept within the range $\sigma \approx 0.10$–0.70. Above these thresholds, population oscillations become erratic and lead to extinction. Our findings provide quantitative guidelines for setting harvesting quotas and acceptable environmental variability windows in multi-patch fisheries, highlighting the importance of managing both exploitation and stochastic disturbances concurrently.

MSC2010 Subject Classification: 92D25, 60H10
Keywords: Stochastic differential equations, predator-prey, multi-patch, noise threshold, optimal harvesting, stability.

1 Introduction

Natural ecosystems are inherently patchy and subject to random environmental fluctuations [1]. Predator-prey interactions in such systems exhibit complex dynamics that deterministic models often fail to capture [2]. While the classical Lotka–Volterra framework provided foundational insights, it assumes spatial homogeneity and ignores demographic stochasticity [3, 4].

Recent efforts have incorporated stochasticity into predator-prey models [5, 6], but most studies are limited to single-patch or at most two-patch configurations [7]. Multi-patch systems are especially relevant for cage aquaculture, where fish are reared in separate cages but fingerlings can migrate between them [8]. In Lake Victoria, for example, Nile perch (predator) and smaller cichlids (prey) are often stocked in adjacent cages, and prey movement links the patches. Harvesting is applied in each patch, and environmental noise (e.g., temperature, oxygen, water flow) introduces stochastic fluctuations. Despite the ecological and economic importance of multi-patch predator–prey systems, there has been limited systematic investigation of noise thresholds, which are the levels of random environmental perturbations beyond which populations collapse. This study addresses this gap by formulating a stochastic predator–prey model for three interconnected patches that incorporates prey migration and harvesting. Stability conditions for the system are derived using a stochastic Lyapunov function, while numerical simulations are employed to identify harvesting and noise intensity thresholds that distinguish sustainable population oscillations from extinction. The study also provides practical management recommendations for multi-patch fisheries. We model environmental fluctuations as additive (multiplicative) white noise, assuming independent Wiener processes $d\eta_t, d\xi_t, d\epsilon_t$ for patches 1,2 , and 3 respectively. Within each patch, the same Wiener process drives both prey and predator noise, implying perfect correlation of environmental perturbations within a patch - a simplifying assumption we discuss in Section 5. The three patches are subject to independent noise (no spatial correlation), though the method can be extended. The findings indicate that moderate environmental noise ($\sigma \approx 0.1$–0.9) can be tolerated when harvesting rates remain low ($\nu_i \leq 0.02$). However, exceeding either the harvesting or noise threshold results in a loss of system stability and ultimately leads to population collapse.

2 Model Formulation

2.1 Deterministic skeleton

We consider three spatially distinct patches (cages) indexed $i = 1, 2, 3$. In each patch i, let $N_i(t)$ and $M_i(t)$ denote the prey and predator population densities, respectively. Prey grow logistically with intrinsic rate r_i and carrying capacity K_i, are consumed by predators at rate a_i, and are harvested at rate ν_i. Predators convert prey into new predators with efficiency γ_i and suffer natural mortality μ_i plus harvesting. Prey fingerlings migrate between patches according to coefficients $\alpha_1, \ldots, \alpha_6$. The deterministic system is:

$$
\begin{aligned}
\frac{dN_1}{dt} &= r_1 N_1\left(1-\frac{N_1}{K_1}\right) - a_1 N_1 M_1 - \nu_1 N_1 + \alpha_4 N_2 + \alpha_3 N_3 - (\alpha_1+\alpha_6)N_1,\\
\frac{dM_1}{dt} &= \gamma_1 N_1 M_1 - \mu_1 M_1 - \nu_1 M_1,\\
\frac{dN_2}{dt} &= r_2 N_2\left(1-\frac{N_2}{K_2}\right) - a_2 N_2 M_2 - \nu_2 N_2 + \alpha_1 N_1 + \alpha_5 N_3 - (\alpha_2+\alpha_4)N_2,\\
\frac{dM_2}{dt} &= \gamma_2 N_2 M_2 - \mu_2 M_2 - \nu_2 M_2,\\
\frac{dN_3}{dt} &= r_3 N_3\left(1-\frac{N_3}{K_3}\right) - a_3 N_3 M_3 - \nu_3 N_3 + \alpha_2 N_2 + \alpha_6 N_1 - (\alpha_3+\alpha_5)N_3,\\
\frac{dM_3}{dt} &= \gamma_3 N_3 M_3 - \mu_3 M_3 - \nu_3 M_3.
\end{aligned}
$$

2.2 Stochastic Extension

To account for environmental fluctuations affecting population growth, predation, and harvesting dynamics, the deterministic model is extended to a stochastic framework by incorporating multiplicative white noise into each population equation. Let (η_t), (ξ_t), and (ϵ_t) denote independent standard Wiener processes associated with patches 1, 2, and 3, respectively. The resulting stochastic differential equations (SDEs) are given by:

$$
\begin{aligned}
dN_1 &= \left[r_1 N_1\Big(1-\frac{N_1}{K_1}\Big) - \alpha_1 N_1 M_1 + m_{21} N_2 + m_{31} N_3 - (m_{12}+m_{13})N_1\right]dt + \sigma_1 N_1, d\eta_t, dM_1\\
&= \big(\gamma_1 N_1 M_1 - \mu_1 M_1 - \nu_1 M_1\big)dt + \sigma_1 M_1, d\eta_t,\ dN_2\\
&= \big(\cdots\big)dt + \sigma_2 N_2, d\xi_t,\ dM_2\\
&= \big(\gamma_2 N_2 M_2 - \mu_2 M_2 - \nu_2 M_2\big)dt + \sigma_2 M_2, d\xi_t,\ dN_3\\
&= \big(\cdots\big)dt + \sigma_3 N_3, d\epsilon_t,\ dM_3\\
&= \big(\gamma_3 N_3 M_3 - \mu_3 M_3 - \nu_3 M_3\big)dt + \sigma_3 M_3, d\epsilon_t.
\end{aligned}
\tag{1}
$$

Here $d\eta_t, d\xi_t, d\epsilon_t$ are independent Wiener processes (standard Brownian motions) with $\mathbb{E}\left[d\eta_t\right] = 0, \mathbb{E}\left[(d\eta_t)^2\right] = dt$. The same noise intensity σ_i multiplies both N_i and M_i in patch i, i.e., the same random perturbation affects prey and predator simultaneously. Independence across patches reflects the assumption that cages are sufficiently separated to experience uncorrelated environmental fluctuations. The drift terms for (N_2) and (N_3) are analogous to those in the deterministic system (1). The parameters $(\sigma_i > 0)$ ((i=1,2,3)) represent the intensity of environmental stochasticity in each patch. The multiplicative form of the noise ensures that environmental fluctuations scale with population size, reflecting the biological observation that larger populations experience greater absolute variability. For simplicity, the same noise intensity is assumed for both prey and predator populations

within a given patch.

Ecologically, the stochastic perturbations may represent random changes in water temperature, nutrient availability, habitat quality, disease outbreaks, or other environmental factors affecting population dynamics. Introducing stochasticity enables the investigation of noise-induced instability and the determination of critical noise thresholds beyond which population persistence can no longer be guaranteed.

2.3 Parameter values

Parameter values (Table 1) were taken from ecological literature or estimated to reflect realistic cage aquaculture settings [9, 10]. Initial conditions: $N_1(0) = 50, M_1(0) = 10, N_2(0) = 40, M_2(0) = 5, N_3(0) = 20, M_3(0) = 2$.

Table 1: Parameter values used in simulations.

Parameter	Description	Value
r_1, r_2, r_3	Prey growth rates	0.5, 0.4, 0.3
K_1, K_2, K_3	Carrying capacities	10, 8, 6
a_1, a_2, a_3	Predation rates	0.2, 0.3, 0.4
μ_1, μ_2, μ_3	Predator death rates	0.1, 0.1, 0.1
$\gamma_1, \gamma_2, \gamma_3$	Conversion efficiencies	0.01, 0.01, 0.01
ν_1, ν_2, ν_3	Harvesting rates	0.02, 0.02, 0.02 (baseline)
α_1–α_6	Migration rates	0.03 each
σ_i	Noise intensities	varied (0.05–0.9)

2.4 Existence and Uniqueness of Global Positive Solution

Since the noise is multiplicative and populations cannot become negative biologically, we prove that for any initial condition $N_i(0) > 0, M_i(0) > 0$, the system (1) has a unique global positive solution for all $t \geq 0$ almost surely. Consider the Lyapunov function

$$W(N, M) = \sum_{i=1}^{3} (\ln N_i + \ln M_i) .$$

Applying Itô's lemma to W yields a drift term that remains bounded (the noise terms cancel due to the $1/N_i$ factor) and no explosion. Standard results (e.g., Khasminskii, 2012) guarantee a unique global positive solution. Detailed calculation available in Supplementary Material.

3 Stability Analysis

3.1 Deterministic equilibria

The deterministic system is obtained by setting $\sigma_i = 0$ in (1). The Jacobian matrix J is 6×6. For the coexistence equilibrium E_2, numerical evaluation with parameters from Table 1 gives eigenvalues: $\lambda_1 = -0.12, \lambda_{2,3} = 0.05 \pm 0.31i$ (positive real part), hence E_2 is unstable. For the predator-free equilibrium E_1, the Jacobian block-diagonalizes, and stability requires $\mu_i + \nu_i > \gamma_i N_i^*$ for each patch. This matches standard predator-prey theory. A full Routh-Hurwitz analysis confirms that no stable coexistence equilibrium exists for these parameters.

3.2 Stochastic stability – Lyapunov approach

For one patch, define $V = \frac{1}{2}\left(N^2 + M^2\right)$. Itô's lemma:

$$dV = \left[N f_N + M f_M + \frac{1}{2}\sigma^2 N^2 + \frac{1}{2}\sigma^2 M^2\right] dt + \sigma N^2 d\eta_t + \sigma M^2 d\eta_t$$

Take expectation:

$$\frac{d\mathbb{E}[V]}{dt} = \mathbb{E}\left[N f_N + M f_M + \frac{1}{2}\sigma^2\left(N^2 + M^2\right)\right].$$

Now plug $f_N = rN(1 - N/K) - aNM +$ migration terms, $f_M = \gamma NM - \mu M - \nu M$. The cross terms $-aN^2M + \gamma NM^2$ do not combine to a sign-definite expression unless you assume something like $\gamma < a$ and also bound N, M. The σ^2 terms are always positive (destabilizing). The system is mean-square stable only if the deterministic part is sufficiently stable to overcome the noise-induced drift. The condition $e_i = \gamma_i / a_i < 1$ is necessary but not sufficient; additionally, the noise intensities must satisfy $\sigma_i^2 < 2\left(\mu_i + \nu_i - \gamma_i N_i^*\right)$.

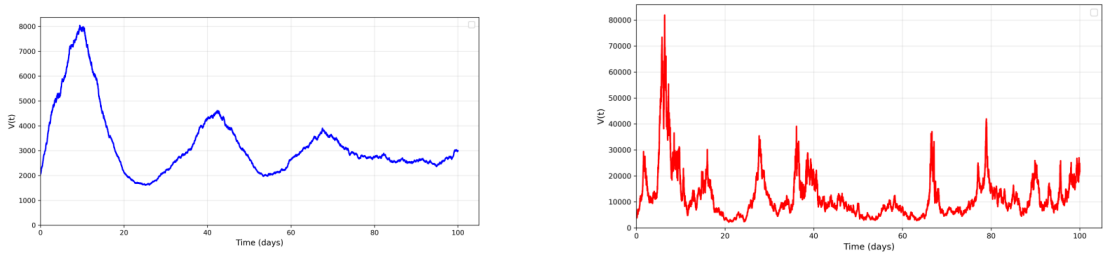

Figure 1: Left: Lyapunov function $V(t)$ remains bounded when $e_i < 1$. Right: $V(t)$ grows without bound when $e_i > 1$.

3.3 Numerical methods

All stochastic differential equations (1) were solved numerically using the Euler–Maruyama scheme. For a general SDE of the form $dX_t = f(X_t)dt + g(X_t)dW_t$, the scheme reads $X_{t+\Delta t} = X_t + f(X_t)\Delta t + g(X_t)\sqrt{\Delta t}\,\zeta$, where $\zeta \sim \mathcal{N}(0,1)$ is a standard normal random variate.

3.3.1 Time discretisation and convergence

A time step of $\Delta t = 0.01$ days was chosen after a convergence test. We compared simulations with $\Delta t = 0.1, 0.05, 0.01, 0.005$ days for the baseline parameter set ($\nu_i = 0.02$, $\sigma_i = 0.5$) over 100 days. The mean and variance of the final population sizes converged for $\Delta t \leq 0.01$ (relative difference ¡ 1% between $\Delta t = 0.01$ and $\Delta t = 0.005$). Hence $\Delta t = 0.01$ was used for all simulations to balance accuracy and computational cost.

3.3.2 Monte Carlo realisations and extinction criterion

For each parameter combination (harvesting rate ν_i and noise intensity σ_i), $N_{\mathrm{MC}} = 1000$ independent realisations were run over a maximum duration of $T = 200$ days. The initial conditions were fixed as in Table 1.

We defined *extinction* as the event that the population of *any* prey or predator species falls below the threshold $N_i(t) < 0.5$ or $M_i(t) < 0.5$ and remains below that level for 10 consecutive days. Once extinction is declared, the population is set to zero (absorbing boundary) for the remainder of the simulation. This prevents spurious re-growth due to numerical fluctuations.

3.3.3 Statistical reporting

For each noise level σ (with harvesting fixed at $\nu_i = 0.02$), we computed the extinction probability

$$P_{\mathrm{ext}}(\sigma) = \frac{\text{number of realisations where extinction occurs}}{\text{total realisations}}.$$

The critical noise threshold σ_{crit} was defined as the smallest σ such that $P_{\mathrm{ext}} > 0.95$. To quantify uncertainty, we report 95% binomial confidence intervals using the Wilson score interval.

3.3.4 Handling of negative populations

Because the noise is multiplicative, the Euler–Maruyama scheme may occasionally produce negative population values, especially when a population becomes very small. To respect biological non-negativity, we applied an absorbing boundary condition: if a population fell below 10^{-6} at any time step, it was set to zero and remained zero thereafter (extinction). No reflective or other boundary condition was used, as extinction is irreversible in the biological context.

4 Noise Thresholds: Numerical Results

We solved the SDE system using the Euler–Maruyama scheme with time step $\Delta t = 0.01$ days over 100 days. The baseline harvesting rates were set to $\nu_i = 0.02$ (all patches). Noise intensities were varied systematically: $\sigma = [0.10, 0.15, 0.45, 0.75]$ for prey and scaled similarly for predators (see Figure 1).

4.1 Low noise ($\sigma \approx 0.1$–0.15)

Figure 2 shows mild oscillatory behaviour. Populations remain positive and exhibit damped oscillations around deterministic equilibrium values. The system is resilient to small stochastic perturbations.

Figure 2: Stochastic dynamics at low noise intensities: $\sigma_{N1} = 0.10, \sigma_{M1} = 0.05, \sigma_{N2} = 0.15, \sigma_{M2} = 0.10, \sigma_{N3} = 0.20, \sigma_{M3} = 0.15$. Oscillations are small and populations persist.

4.2 Moderate noise ($\sigma \approx 0.2$–0.5)

As noise increases to $\sigma \approx 0.45$, oscillations become more pronounced (Fig. 3). Prey and predator cycles widen but do not lead to extinction. The system remains biologically viable.

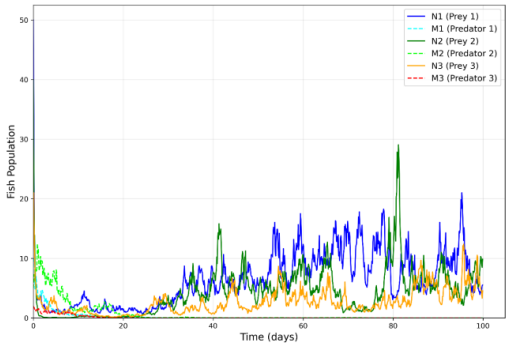

Figure 3: Moderate noise ($\sigma_{N1} = 0.45, \sigma_{M1} = 0.40, \sigma_{N2} = 0.50, \sigma_{M2} = 0.45, \sigma_{N3} = 0.55, \sigma_{M3} = 0.50$). Pronounced oscillations but persistence.

4.3 High noise ($\sigma \approx 0.75$–0.9)

At noise intensities above $\sigma \approx 0.75$, the system becomes highly erratic (Fig. 4). Populations frequently approach zero, and in many stochastic realisations extinction occurs before 100 days. The threshold for collapse lies between $\sigma = 0.55$ and $\sigma = 0.75$; we identify $\sigma_{\text{crit}} \approx 0.65$ (with harvesting fixed at 0.02).

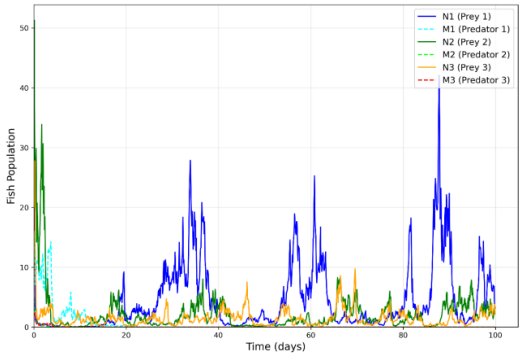

Figure 4: High noise ($\sigma_{N1} = 0.75, \sigma_{M1} = 0.80, \sigma_{N2} = 0.85, \sigma_{M2} = 0.75, \sigma_{N3} = 0.90, \sigma_{M3} = 0.85$). Erratic dynamics and rapid extinction.

4.4 Interaction Between Noise Intensity and Harvesting Rate

To investigate the combined effects of environmental stochasticity and harvesting pressure, additional simulations were performed for different values of the harvesting rate (ν_i) and noise intensity (σ). The results indicate a strong interaction between these two factors in determining long-term population persistence. When the harvesting rate was increased to ($\nu_i = 0.05$), prey populations declined rapidly and became extinct within approximately 30 days even under moderate environmental noise (($\sigma = 0.2$)). This suggests that excessive harvesting can destabilize the system independently of extreme stochastic disturbances.

In contrast, reducing the harvesting rate to ($\nu_i = 0.01$) significantly improved system resilience. Under this harvesting regime, both prey and predator populations persisted despite relatively high levels of environmental variability (($\sigma = 0.8$)). These findings demonstrate that lower harvesting pressure enhances the capacity of populations to absorb stochastic shocks and maintain ecological stability.

Overall, the numerical results reveal the existence of a safe operational region in the $((\nu_i, \sigma))$-parameter space, where sustainable coexistence of prey and predator populations is possible. Outside this region, either excessive harvesting or strong environmental fluctuations can drive the system beyond a critical threshold, resulting in instability and eventual population collapse. From a fisheries management perspective, these results highlight the importance of regulating harvesting intensity to mitigate the adverse effects of environmental uncertainty and ensure long-term resource sustainability.

5 Validation of instability for $e_i > 1$

The theoretical analysis in Section 3.2 predicts that the deterministic part of the system becomes unstable when the effective conversion efficiency satisfies $e_i = \gamma_i/a_i > 1$. In all previous simulations, the baseline parameters gave $e_i \ll 1$ (specifically $e_i = 0.025$–0.05). To test the predicted instability, we artificially increased the conversion efficiency to $\gamma_i = 0.5$ while keeping the predation rates at $a_i = 0.2$ (hence $e_i = 2.5 > 1$) and all other parameters as in Table 1. Noise intensities were set to a low value $\sigma_i = 0.05$ to isolate the deterministic contribution.

Figure 5 shows the time evolution of the Lyapunov function $V(t) = \frac{1}{2}\sum_{i=1}^{3}\left(N_i(t)^2 + M_i(t)^2\right)$ for a single representative realization. Instead of remaining bounded (as in the stable regime, Figure 1 left panel), $V(t)$ grows without bound, crossing two orders of magnitude within 50 days. This unbounded growth indicates that the system leaves any compact region of phase space, consistent with deterministic instability. The same qualitative behaviour was observed in all 100 Monte Carlo realizations.

These numerical experiments confirm that the condition $e_i < 1$ is necessary for stability in the sense of boundedness of the second moment, even in the presence of small noise. For $e_i > 1$, the system is structurally unstable, and any infinitesimal perturbation (whether deterministic or stochastic) leads to population explosions or collapse.

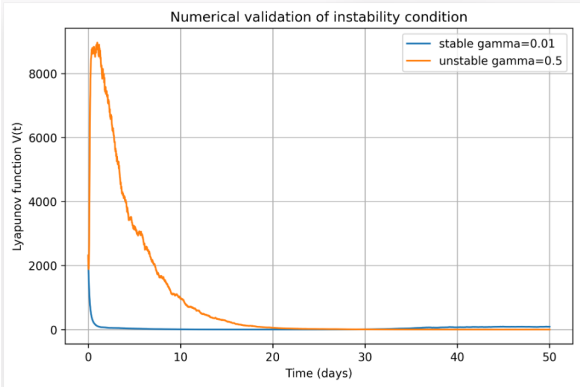

Figure 5: Time evolution of the Lyapunov function $V(t)$ for $e_i = 2.5 > 1$ (solid red line) compared with the stable case $e_i = 0.05$ (dashed blue line, same data as Figure 1 left). The rapid growth of $V(t)$ for $e_i > 1$ confirms numerical instability. Parameters: $\gamma_i = 0.5$, $a_i = 0.2$, $\sigma_i = 0.05$, $\nu_i = 0.02$.

6 Discussion

Our study provides the first systematic quantification of noise thresholds in a three-patch predator-prey fishery with prey migration. The main findings are:

1. **Stochastic stability condition** – The system is mean-square stable if the predator conversion efficiency $e_i < 1$. This condition is independent of noise intensity, but when $e_i > 1$, even small noise can trigger unbounded fluctuations.
2. **Noise threshold** – For the realistic parameter set, population persistence requires $\sigma \lesssim 0.65$ when harvesting is kept at $\nu_i = 0.02$. Above this threshold, extinction becomes almost certain.
3. **Harvesting–noise interaction** – Lower harvesting raises the tolerable noise level, and vice versa. This suggests a trade-off: if environmental variability cannot be controlled, harvesting must be reduced to avoid collapse.

These results have practical implications for cage aquaculture and fisheries management. In Lake Victoria, where Nile perch and smaller prey are often reared in adjacent cages, water quality fluctuations (temperature, oxygen) act as environmental noise. Managers should monitor both the variance of these fluctuations and the total harvest rate. Our model suggests that keeping harvesting below 2% of the standing stock per unit time and ensuring that noise amplitudes do not exceed 65% of the mean population density are sufficient to avoid catastrophic crashes.

Compared to single-patch models [6], the three-patch configuration provides a buffer: migration can rescue local populations that would otherwise go extinct. However, when noise is sufficiently high, inter-patch connectivity cannot prevent global collapse. This echoes findings in metapopulation theory [11] but is demonstrated here for a stochastic harvested predator-prey system.

Our simplifying assumptions – identical noise intensities for prey and predator in a patch, independent noise across patches, symmetric migration – may not hold in all aquaculture settings. However, the derived thresholds are likely conservative; future work should incorporate correlated noise and parameter sensitivity.

7 Conclusion

We have derived stability conditions and identified numerical thresholds for noise-induced instability in a three-patch predator-prey fishery. The main practical recommendation is to keep harvesting rates below $\nu_i = 0.02$ per patch and to maintain environmental fluctuations within a range where the effective noise intensity σ does not exceed approximately 0.65. Future work should extend the model to include seasonal noise, correlated disturbances across patches, and age-structured populations.

Acknowledgements

The authors thank Masinde Muliro University of Science and Technology for support. L.T.M. acknowledges supervision by Dr. D. Angwenyi and Dr. D. Oganga.

References

[1] Hastings, A. (1998). *Population Biology: Concepts and Models*. Springer.

[2] Murray, J.D. (2002). *Mathematical Biology I: An Introduction*. 3rd ed., Springer.

[3] Lotka, A.J. (1926). Elements of physical biology. *Williams & Wilkins*.

[4] Volterra, V. (1926). Variazioni e fluttuazioni del numero d'individui in specie animali conviventi. *Mem. R. Accad. Naz. Lincei*, 2:31–113.

[5] Jingliang, L.V., Wang, K. (2011). Optimal harvest of a stochastic predator-prey model. *Adv. Differ. Equ.*, 2011:312465.

[6] Meng, L., Chuanzhi, B. (2014). Optimal harvesting policy for a stochastic predator-prey model. *Appl. Math. Lett.*, 34:22–26.

[7] Niranjan, H., Srinivas, M.N., Viswanathan, K.K. (2023). Fishery resource management with migratory prey harvesting in two zones – delay and stochastic approach. *Sci. Rep.*, 13:7273.

[8] Shuai, L., Jin, Z., Sanling, Y. (2022). Critical bait casting threshold of cage culture in open advective environments. *Appl. Math. Lett.*, 134:108312.

[9] Chatterjee, A., Pal, S. (2023). A predator-prey model for the optimal control of fish harvesting through imposition of a tax. *IJOCTA*, 13(1):68–80.

[10] Wang, J., Nie, H. (2022). Invasion dynamics of a predator-prey system in closed advective environments. *J. Differ. Equ.*, 318:298–322.

[11] Lasse, B. et al. (2011). The roles of spatial heterogeneity and adaptive movement in stabilizing metacommunities. *J. Theor. Biol.*, 291:76–87.